Chapter 5

Solving the EMI Equations using Finite Element Methods

Miroslav Kuchta[1], Kent-André Mardal[1,2] and Marie E. Rognes[1]

Abstract This chapter discusses 2×2 symmetric variational formulations and associated finite element methods for the EMI equations. We demonstrate that the presented methods converge at expected rates, and compare the approaches in terms of approximation of the transmembrane potential. Overall, the choice of which formulation to employ for solving EMI models becomes largely a matter of desired accuracy and available computational resources.

5.1 Introduction

In this chapter, we present different weak formulations and corresponding finite element methods for solving the EMI equations as presented in (7, Chapter 1) over a physiological cell Ω_i and its membrane Γ surrounded by an extracellular space Ω_e and a time interval $(0, T]$ for some time $T > 0$. This coupled, time-dependent, and typically nonlinear system of equations can be targeted numerically by an operator splitting scheme, see e.g (8, Chapter 4). Such an approach, combined with for instance an implicit Euler discretization in time, gives the following stationary and linear, but still coupled system of equations to be solved at each time-step: find the potentials $u_e = u_e(x)$, $u_i = u_i(x)$ (and current $I_m = I_m(x)$) such that

[1]Simula Research Laboratory, Norway
[2]Department of Mathematics, University of Oslo, Oslo, Norway

A. Tveito et al. (eds.), *Modeling Excitable Tissue*, Simula SpringerBriefs on Computing 7, https://doi.org/10.1007/978-3-030-61157-6_5

$$-\nabla \cdot (\sigma_e \nabla u_e) = 0 \qquad \text{in } \Omega_e, \tag{5.1a}$$
$$-\nabla \cdot (\sigma_i \nabla u_i) = 0 \qquad \text{in } \Omega_i \tag{5.1b}$$
$$\sigma_e \nabla u_e \cdot \boldsymbol{n}_e = -\sigma_i \nabla u_i \cdot \boldsymbol{n}_i \equiv I_m \qquad \text{on } \Gamma, \tag{5.1c}$$
$$u_i - u_e = v \qquad \text{on } \Gamma, \tag{5.1d}$$
$$v - C_m^{-1} \Delta t I_m = f \qquad \text{on } \Gamma, \tag{5.1e}$$

where $\Delta t > 0$ denotes a time step size, and $\boldsymbol{n}_e$ (resp. $\boldsymbol{n}_i$) denotes the outward pointing normal on Γ when viewed from Ω_e (resp. Ω_i). In our (implicit Euler) time discretization context, the known right-hand side f of (5.1e) combines the previous transmembrane potential solution, v_0, and the evaluation of the ionic current, I_{ion}, into $f \equiv v_0 - C_m^{-1} \Delta t I_{\text{ion}}$.

We assume that the potential is grounded on part of the external boundary Γ_e^D and that the remaining external boundary Γ_e^N is insulated. These assumptions give the boundary conditions:

$$u_e = 0 \qquad \text{on } \Gamma_e^D, \tag{5.2a}$$
$$\sigma_e \nabla u_e \cdot \boldsymbol{n}_e = 0 \qquad \text{on } \Gamma_e^N. \tag{5.2b}$$

This geometrical setting is illustrated in Figure 5.1.

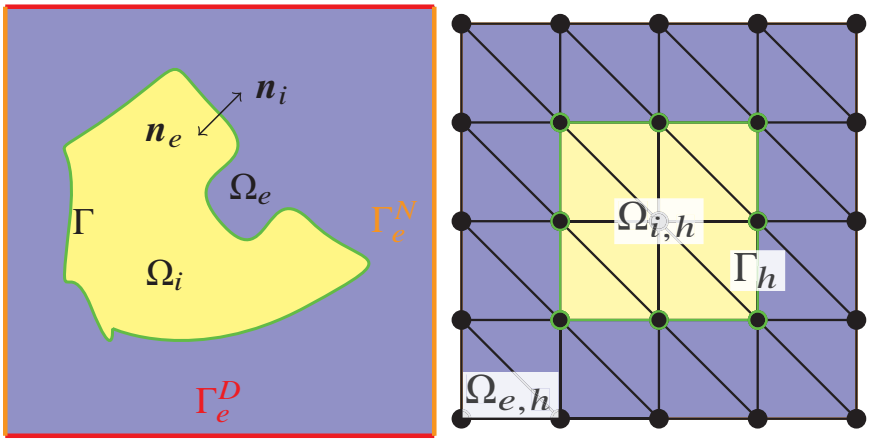

Fig. 5.1: (Left) Illustration of the geometric setting for the single cell EMI problem. (Right) Sample meshes for our benchmark problem (5.17). The boundary facets of the intracellular mesh $\Omega_{i,h}$ form the membrane mesh Γ_h.

Remark 5.1 We remark that a single cell model is here considered for simplicity. Indeed the formulations to be studied below can be similarly derived for the intercalated

model (collections of connected cells). Formulations for a number of disconnected cells are then practically identical to the case considered here.

Remark 5.2 If (5.2) is considered without any Dirichlet boundary data, i.e. $|\Gamma_e^D| = 0$, then only the transmembrane potential is fixed and the intracellular and extracellular potentials are determined only up to a single, common constant.

The EMI equations (5.1) set a rich scene for numerical exploration and can be solved in a multitude of ways. In this chapter, we will derive 2×2 different weak formulations (each defining a finite element method) of this system. The two first formulations (in Section 5.2) compute the intracellular and extracellular potentials as the main unknowns. These are referred to as *primal formulations*. The latter two formulations (in Section 5.3) additionally introduce the current densities $\boldsymbol{J}_i = -\sigma_i \nabla u_i$ and $\boldsymbol{J}_e = -\sigma_e \nabla u_e$ as independent unknowns. These are referred to as *mixed formulations*. We compare finite element discretizations of the primal and mixed formulations with respect to the approximation of the transmembrane potential v in Section 5.4. This choice is motivated by the observation that v is closely coupled to the membrane dynamics as discussed in Chapter 1.

5.1.1 Preliminaries: Function Spaces and Norms

The EMI equations (5.1) define a multi-dimensional[1] PDE system coupling unknown fields defined over cellular domains and fields defined over the cell membrane, which can be viewed as a lower-dimensional manifold. Identifying the right function spaces for the different unknown fields is key to defining well-posed weak formulations of these equations. We here present suitable Sobolev spaces for this setting; the reader is referred to e.g. (3; 5) for more material and careful formalizations.

Let Ω be a bounded, polygonal domain in $\mathbb{R}^d$ for $d = 2, 3$. We denote the space of square-integrable functions over Ω by $L^2(\Omega)$, and let $H^1(\Omega)$ be the Sobolev space of functions in $L^2(\Omega)$ with weak derivatives in $L^2(\Omega)$. The space $\boldsymbol{H}(\mathrm{div}, \Omega)$ contains vector-valued functions $\boldsymbol{v} : \Omega \to \mathbb{R}^d$ such that $\boldsymbol{v} \in \boldsymbol{L}^2(\Omega)$ and $\nabla \cdot \boldsymbol{v} \in L^2(\Omega)$. In general, when clear from the context, the domain will be omitted from the notation.

The L^2-inner product and norm for $u, v \in L^2(\Omega)$ is written as

$$(u, v)_{0,\Omega} = \int_\Omega uv \, \mathrm{d}x, \quad \|v\|_{0,\Omega}^2 = \int_\Omega v^2 \, \mathrm{d}x.$$

Similarly, we define the H^1-norm as $\|v\|_{1,\Omega}^2 = \|v\|_{0,\Omega}^2 + \|\nabla v\|_{0,\Omega}^2$ for $v \in H^1(\Omega)$, and the $\boldsymbol{H}(\mathrm{div})$-norm as $\|\boldsymbol{v}\|_{\mathrm{div},\Omega}^2 = \|\boldsymbol{v}\|_{0,\Omega}^2 + \|\nabla \cdot \boldsymbol{v}\|_{0,\Omega}^2$.

[1] PDEs coupling fields over domains of different topological dimensions are often referred to as mixed-dimensional PDEs. To avoid the confusion-inducing term mixed-dimensional mixed in the subsequent sections, we instead use the term multi-dimensional in this chapter.

For $\Gamma \subseteq \partial\Omega$, we define the constrained spaces $H^1_\Gamma(\Omega) = \left\{v \in H^1(\Omega) \mid v = 0 \text{ on } \Gamma\right\}$, and $\boldsymbol{H}_\Gamma(\mathrm{div}, \Omega) = \{\boldsymbol{v} \in \boldsymbol{H}(\mathrm{div}, \Omega) \mid \boldsymbol{v} \cdot \boldsymbol{n} = 0 \text{ on } \Gamma\}$ where $\boldsymbol{n}$ is the (outward pointing) normal vector of Γ. Finally the spaces $H^{1/2}(\Gamma)$ and $H^{-1/2}(\Gamma)$ are the trace spaces of H^1 and $\boldsymbol{H}(\mathrm{div})$ respectively (6, Ch. 1., 2.). Here, the spaces will be considered with the norm defined in terms of fractional powers of the Helmholtz operator, see e.g. (4), i.e.

$$\|u\|_s^2 = (u, (-\Delta + I)^s u)_{0,\Gamma}, \; u \in C^\infty(\Gamma).$$

We remark that in the following experiments the fractional norm is evaluated using the eigenvalue decomposition of $-\Delta + I$ as detailed in (11).

5.2 Primal Formulations

We present two primal formulations of the stationary EMI system (5.1) with the boundary conditions given by (5.2): one *single-dimensional* formulation and one *multi-dimensional* formulation. The difference in the intra- and extracellular potential across the cell membrane Γ sets up a potential jump, the transmembrane potential v, c.f. (5.1d). Due to this jump, one cannot define a global, differentiable potential $u \in H^1(\Omega_i \cup \Omega_e)$ such that $u|_{\Omega_i} = u_i$ and $u|_{\Omega_e} = u_e$. Instead, we seek $u_i \in H^1(\Omega_i)$ and $u_e \in H^1(\Omega_e)$ separately. In the single-dimensional formulation, these are the only unknown fields, while in the multi-dimensional formulation, we keep I_m as an additional unknown.

5.2.1 Single-Dimensional Primal Formulation

Define the function spaces

$$V_i = H^1(\Omega_i), \quad V_e = H^1_{\Gamma_e^D}(\Omega_e). \tag{5.3}$$

To derive a weak formulation of (5.1), multiply (5.1a) by a test function $v_e \in V_e$, (5.1b) by another test function $v_i \in V_i$, and integrate the divergence by parts. This yields the variational formulation: find $u_e \in V_e$, $u_i \in V_i$ satisfying

$$\int_{\Omega_e} \sigma_e \nabla u_e \cdot \nabla v_e \, \mathrm{d}x - \int_\Gamma \sigma_e \nabla u_e \cdot \boldsymbol{n}_e v_e \, \mathrm{d}s = 0, \tag{5.4a}$$

$$\int_{\Omega_i} \sigma_i \nabla u_i \cdot \nabla v_i \, \mathrm{d}x + \int_\Gamma (-\sigma_i \nabla u_i \cdot \boldsymbol{n}_i) \, v_i \, \mathrm{d}s = 0. \tag{5.4b}$$

for all $v_e \in V_e$, $v_i \in V_i$. In the bracketed term of (5.4b), we recognize the membrane current density I_m as defined by (5.1c), and similarly, the interface contribution in

the corresponding extracellular equation (5.4a) hides $-I_m$. Combining (5.1e) and (5.1d), we find that

$$I_m = C_m(\Delta t)^{-1}\left((u_i - u_e) - f\right). \tag{5.5}$$

After substituting (5.5) into (5.4), the single-dimensional primal weak form of (5.1) reads: find $u_i \in V_i$ and $u_e \in V_e$ such that

$$\begin{aligned}
\int_{\Omega_e} \sigma_e \nabla u_e \cdot \nabla v_e \,\mathrm{d}x + \int_\Gamma C_m(\Delta t)^{-1} u_e v_e \,\mathrm{d}s - \int_\Gamma C_m(\Delta t)^{-1} u_i v_e \,\mathrm{d}s = \\
- C_m(\Delta t)^{-1} \int_\Gamma f v_e \,\mathrm{d}s, \\
\int_{\Omega_i} \sigma_i \nabla u_i \cdot \nabla v_i \,\mathrm{d}x + \int_\Gamma C_m(\Delta t)^{-1} u_i v_i \,\mathrm{d}s - \int_\Gamma C_m(\Delta t)^{-1} u_e v_i \,\mathrm{d}s = \\
C_m(\Delta t)^{-1} \int_\Gamma f v_i \,\mathrm{d}s,
\end{aligned} \tag{5.6}$$

for all $v_e \in V_e$ and $v_i \in V_i$.

We remark that (5.6) can be viewed as a coupling of two Poisson problems with a Robin boundary condition on Γ. The well-posedness of the problem is then discussed in (10, Chapter 6). Finally, the transmembrane potential can here be computed from its definition (5.1d) as a difference of the computed potentials.

5.2.2 Multi-Dimensional Primal Formulation

An alternative formulation can be derived by keeping I_m as a separate unknown field. Since Γ is of a different (lower) dimension than Ω_i, Ω_e; and as $I_m : \Gamma \to \mathbb{R}$ while $u_i : \Omega_i \to \mathbb{R}$, $u_e : \Omega_e \to \mathbb{R}$, we will refer to this as a multi-dimensional primal formulation. Observe that (5.4) now yields two equations for three unknowns $u_i \in V_i$, $u_e \in V_e$, and $I_m \in Q$:

$$\begin{aligned}
\int_{\Omega_e} \sigma_e \nabla u_e \cdot \nabla v_e \,\mathrm{d}x - \int_\Gamma I_m v_e \,\mathrm{d}s = 0, \quad \forall\, v_e \in V_e, \\
\int_{\Omega_i} \sigma_i \nabla u_i \cdot \nabla v_i \,\mathrm{d}x + \int_\Gamma I_m v_i \,\mathrm{d}s = 0, \quad \forall\, v_i \in V_i.
\end{aligned}$$

However, the missing equation can be obtained from (5.5). Let

$$Q = H^{1/2}(\Gamma), \quad Q^* = H^{-1/2}(\Gamma). \tag{5.7}$$

We remind the reader that if Γ is a co-dimensional 1 subset of Ω then trace operations from Ω to Γ, $Tu = u|_\Gamma$, $u \in C(\Omega)$ and $T_n\boldsymbol{\tau} = \boldsymbol{\tau}|_\Gamma \cdot \boldsymbol{n}$, $\boldsymbol{\tau} \in \boldsymbol{C}(\Omega)$, formally have the following mapping properties $T : H^1(\Omega) \to H^{1/2}(\Gamma)$ and $T_n : \boldsymbol{H}(\mathrm{div}, \Omega) \to$

$H^{-1/2}(\Gamma)$. Hence, let j_m be a a test function from Q^*. We shall then enforce that (5.5) holds in the weak sense:

$$\int_\Gamma (u_i - u_e) j_m \,\mathrm{d}s - \int_\Gamma \Delta t C_m^{-1} I_m j_m \,\mathrm{d}s = \int_\Gamma f j_m \,\mathrm{d}s, \quad \forall\, j_m \in Q^*.$$

In turn, the multi-dimensional primal formulation of (5.1) reads: find $u_i \in V_i$, $u_e \in V_e$, $I_m \in Q^*$ such that

$$\begin{aligned} \int_{\Omega_e} \sigma_e \nabla u_e \cdot \nabla v_e \,\mathrm{d}x - \int_\Gamma v_e I_m \,\mathrm{d}s &= 0, \\ \int_{\Omega_i} \sigma_i \nabla u_i \cdot \nabla v_i \,\mathrm{d}x + \int_\Gamma v_i I_m \,\mathrm{d}s &= 0, \\ \int_\Gamma -u_e j_m \,\mathrm{d}s + \int_\Gamma u_i j_m \,\mathrm{d}s - \int_\Gamma \Delta t C_m^{-1} I_m j_m \,\mathrm{d}s &= \int_\Gamma f j_m \,\mathrm{d}s, \end{aligned} \tag{5.8}$$

for all $v_i \in V_i$, $v_e \in V_e$ and $j_m \in Q^*$. We remark that (5.8) is closely related to the Babuška problem for enforcing boundary conditions by Lagrange multipliers (1) and the mortar finite element method, see e.g. (13). With regards to evaluation of the transmembrane potential, we note that v can be post-computed in several ways: from (5.1d) (as for the single-dimensional primal formulation (5.6)) or from I_m and (5.1e).

5.3 Mixed Formulations

We now turn to consider *mixed formulations* of the EMI system (5.1). Let us (re)introduce the current densities

$$\boldsymbol{J}_i = -\sigma_i \nabla u_i, \quad \boldsymbol{J}_e = -\sigma_e \nabla u_e \tag{5.9}$$

and the global field $\boldsymbol{J}$ on $\Omega = \Omega_i \cup \Omega_e$ such that $\boldsymbol{J}|_{\Omega_i} = \boldsymbol{J}_i$ and $\boldsymbol{J}|_{\Omega_e} = \boldsymbol{J}_e$. In general, we use the convention that for a scalar or vector field u defined on Ω, the restriction on Ω_i and Ω_e is denoted by u_i and u_e, respectively.

With these definitions, (5.1a)–(5.1c) become: find the current densities $\boldsymbol{J}_i, \boldsymbol{J}_e$ (or $\boldsymbol{J}$) and the potentials u_i, u_e (or u) satisfying

$$\sigma_e^{-1} \boldsymbol{J}_e + \nabla u_e = 0 \qquad \text{on } \Omega_e, \tag{5.10a}$$

$$\sigma_i^{-1} \boldsymbol{J}_i + \nabla u_i = 0 \qquad \text{on } \Omega_i, \tag{5.10b}$$

$$-\nabla \cdot \boldsymbol{J} = 0 \qquad \text{in } \Omega, \tag{5.10c}$$

$$\boldsymbol{J}_e \cdot \boldsymbol{n}_e + \boldsymbol{J}_i \cdot \boldsymbol{n}_i = 0 \qquad \text{on } \Gamma. \tag{5.10d}$$

We refer to (5.10) together with (5.1d)–(5.1e) as the mixed EMI system with boundary conditions given by (5.2). Weak formulations of the mixed form can enjoy improved conservation properties and stability properties (3). In particular, approximations of $\boldsymbol{J}$ may be computed such that they are exactly divergence free, cf. (5.10c).

The continuity condition (5.10d) ensures that the normal component of $\boldsymbol{J}$ is continuous on Γ. We remark that $\boldsymbol{v} \in \boldsymbol{H}(\mathrm{div}, \Omega)$ implies continuity of $\boldsymbol{v} \cdot \boldsymbol{n}$ on Γ. Moreover, we observe that (5.10c) involves only divergence of the field $\boldsymbol{J}$. It is therefore sufficient to seek $\boldsymbol{J}$ in $S = \boldsymbol{H}_{\Gamma_e^N}(\mathrm{div}, \Omega)$. Note that in contrast to the primal formulation, here the Neumann boundary condition (5.2b) is enforced as an essential condition; that is, it is included in the construction of the function space S.

5.3.1 Single-Dimensional Mixed Formulation

Let

$$S = \left\{ \boldsymbol{J} \in \boldsymbol{H}_{\Gamma_e^N}(\mathrm{div}, \Omega); \boldsymbol{J} \cdot \boldsymbol{n} \in L^2(\Gamma) \right\}, \quad V = L^2(\Omega). \tag{5.11}$$

To derive a weak form of the mixed EMI system, consider a test function $\boldsymbol{\tau} \in S$. Taking the dot product of (5.10a), (5.10b) with $\boldsymbol{\tau}_i$, $\boldsymbol{\tau}_e$, integrating and applying integration by parts then yields

$$\begin{aligned} \int_{\Omega_e} \sigma_e^{-1} \boldsymbol{J}_e \cdot \boldsymbol{\tau}_e \, \mathrm{d}x - \int_{\Omega_e} u_e \nabla \cdot \boldsymbol{\tau}_e \, \mathrm{d}x + \int_{\Gamma} u_e \boldsymbol{\tau}_e \cdot \boldsymbol{n}_e \, \mathrm{d}s = - \int_{\Gamma_e^D} u_e \boldsymbol{\tau}_e \cdot \boldsymbol{n}_e \, \mathrm{d}s, \\ \int_{\Omega_i} \sigma_i^{-1} \boldsymbol{J}_i \cdot \boldsymbol{\tau}_i \, \mathrm{d}x - \int_{\Omega_i} u_i \nabla \cdot \boldsymbol{\tau}_i \, \mathrm{d}x + \int_{\Gamma} u_i \boldsymbol{\tau}_i \cdot \boldsymbol{n}_i \, \mathrm{d}s = 0. \end{aligned}$$

Observe that by continuity of the normal component of the test function ($\boldsymbol{\tau}_i \cdot \boldsymbol{n} = \boldsymbol{\tau}_e \cdot \boldsymbol{n}$ on Γ), and the identity $\boldsymbol{n}_e = -\boldsymbol{n}_i$, the integrals on Γ can be added, resulting in $\int_\Gamma (u_i - u_e) \boldsymbol{\tau} \cdot \boldsymbol{n}_i$. Moreover, using (5.5), the membrane term can be rewritten as $\int_\Gamma \left(C_m^{-1} \Delta t \boldsymbol{J} \cdot \boldsymbol{n}_i + f \right) \boldsymbol{\tau} \cdot \boldsymbol{n}_i$. In turn, we arrive at the variational problem: find $\boldsymbol{J} \in S$, $u \in V$ such that

$$\begin{aligned} \int_\Omega \sigma^{-1} \boldsymbol{J} \cdot \boldsymbol{\tau} \, \mathrm{d}x + \int_\Gamma C_m^{-1} \Delta t \boldsymbol{J} \cdot \boldsymbol{n}_i \boldsymbol{\tau} \cdot \boldsymbol{n}_i \, \mathrm{d}s - \int_\Omega u \nabla \cdot \boldsymbol{\tau} \, \mathrm{d}x = - \int_\Gamma f \boldsymbol{\tau} \cdot \boldsymbol{n}_i \, \mathrm{d}s, \\ - \int_\Omega q \nabla \cdot \boldsymbol{J} \, \mathrm{d}x = 0, \end{aligned} \tag{5.12}$$

for all $\boldsymbol{\tau} \in S$ and $q \in V$, with σ defined naturally as $\sigma|_{\Omega_i} = \sigma_i$ and likewise for Ω_e. Note that due to the extra trace regularity of the trial/test space S all the terms in (5.12), and in particular the interface term $\int_\Gamma C_m^{-1} \Delta t \boldsymbol{J} \cdot \boldsymbol{n}_i \boldsymbol{\tau} \cdot \boldsymbol{n}_i \, \mathrm{d}s$, are well defined. Without the extra regularity, i.e. if $S = \boldsymbol{H}_{\Gamma_e^N}(\mathrm{div}, \Omega)$, this would not be the case.

We remark that (5.12) is a Γ-perturbed mixed formulation of the Poisson problem (see e.g. (3; 9) for more details on mixed formulations of the Poisson problem).

Considering the task of approximating the transmembrane potential, we observe that v can be computed in two ways, as for the multi-dimensional primal formulation. Indeed, in addition to the identity $v = u_i - u_e$, cf. (5.1d), equation (5.1e) can be used since $I_m = \boldsymbol{J} \cdot \boldsymbol{n}_i$ is readily available.

5.3.2 Multi-Dimensional Mixed Formulation

As for the primal formulations, the multi-dimensional mixed formulation is obtained by keeping the interface term as an explicit unknown field. Let

$$S = \boldsymbol{H}_{\Gamma_e^N}(\mathrm{div}, \Omega), \quad V = L^2(\Omega), \quad W = H^{1/2}(\Gamma). \tag{5.13}$$

To complete the formulation, the equation to be enforced weakly by test functions $w \in W$ is the membrane dynamics condition (5.1e) written in the form

$$\boldsymbol{J} \cdot \boldsymbol{n}_i - C_m(\Delta t)^{-1} v = -C_m(\Delta t)^{-1} f \quad \text{on } \Gamma.$$

The final multi-dimensional mixed weak formulation then reads: Find the current densities $\boldsymbol{J} \in S$, potentials $u \in V$, and transmembrane potential $v \in W$ such that

$$\begin{aligned} \int_\Omega \sigma^{-1} \boldsymbol{J} \cdot \boldsymbol{\tau} \,\mathrm{d}x - \int_\Omega u \nabla \cdot \boldsymbol{\tau} \,\mathrm{d}x + \int_\Gamma v \boldsymbol{\tau} \cdot \boldsymbol{n}_i \,\mathrm{d}s &= 0, \\ - \int_\Omega q \nabla \cdot \boldsymbol{J} \,\mathrm{d}x &= 0, \\ \int_\Gamma w \boldsymbol{J} \cdot \boldsymbol{n}_i \,\mathrm{d}s - \int_\Gamma C_m(\Delta t)^{-1} v w \,\mathrm{d}s &= -C_m(\Delta t)^{-1} \int_\Gamma f w \,\mathrm{d}s, \end{aligned} \tag{5.14}$$

for all $\boldsymbol{\tau} \in S$, $q \in V$ and $w \in W$. Note that (5.14) is defined on the standard $\boldsymbol{H}(\mathrm{div})$ space, cf. (5.12), as the formulation no longer contains the troublesome interface term $\int_\Gamma C_m^{-1} \Delta t \boldsymbol{J} \cdot \boldsymbol{n}_i \boldsymbol{\tau} \cdot \boldsymbol{n}_i \,\mathrm{d}s$. With regards to the approximation of v in formulation (5.14), observe that no post-processing is required to obtain this quantity. This is contrast to the previous three formulations. We remark that (5.14) is closely connected to the Babuška problem for the mixed Poisson equation (2).

5.4 Finite Element Spaces and Methods

To solve the primal and mixed, single- and multi-dimensional weak formulations numerically, we approximate the continuous function spaces by discrete finite element spaces. Each choice of formulation and finite element space defines a finite element method for solving the EMI system.

Now, let Ω_h be a mesh of the domain $\Omega = \Omega_i \cup \Omega_e$ with characteristic mesh size h, which conforms to Γ in the sense that no element of Ω_h has its interior intersected by Γ. The meshes $\Omega_{e,h}$ and $\Omega_{i,h}$ of the extracellular and intracellular domains are formed as non-overlapping subsets of the cells of Ω_h. As a consequence, the mesh Γ_h of Γ is formed by the facets of elements of Ω_h, cf. Figure 5.1. We remark that the single-dimensional primal formulation allows for independent discretizations of Ω_i, Ω_e as well as Γ.

The choice of the finite element spaces plays a crucial role for the stability of the different discrete formulations. In particular, for the saddle-point systems, the spaces must be compatible in the sense of Babuška-Brezzi and satisfy discrete inf-sup conditions, see e.g. (3). For the primal formulations (5.4) and (5.8), we seek discrete unknowns and test functions in

$$V_{i,h} = P_1(\Omega_{i,h}) \subset V_i, \quad V_{e,h} = P_1(\Omega_{e,h}) \subset V_e, \quad Q_h = P_1(\Gamma_h) \subset Q, \tag{5.15}$$

where P_1 denotes the space of continuous piecewise linears (defined relative to the relevant mesh). With these spaces, we expect linear convergence with the mesh size h for all variables in H^1-norms and quadratic convergence in the L^2-norm.

For the mixed formulations (5.10) and (5.12), we seek discrete unknowns and test functions in

$$S_h = RT_0(\Omega_h) \subset S, \quad V_h = P_0(\Omega_h) \subset V, \quad W_h = P_0(\Gamma_h). \tag{5.16}$$

Here RT_0 denotes the lowest order Raviart-Thomas finite element spaces and P_0 denotes the space of piecewise constants defined relative to the relevant mesh. These spaces satisfy the relevant stability conditions, and we expect linear convergence of all unknown fields in their respective natural norms.

5.5 Numerical Results

5.5.1 Comparison of Convergence between Formulations

In order to compare the properties of the different formulations, and in particular their numerical stability and accuracy, we consider a manufactured solution test case with a smooth analytical solution. We define $\Omega = [0,1]^2$ and $\Omega_i = [0.25, 0.75]^2$ with $|\Gamma_e^N| = 0$. For simplicity, let $\sigma_i = 1$, $\sigma_e = 2$, $C_m = 1$, $\Delta t \in \left\{1, 10^{-4}\right\}$ and consider the exact solution

$$\begin{aligned} u_e &= \sin\left(\pi(x+y)\right), \\ u_i &= \tfrac{u_e}{\sigma_i} + \cos\left(\pi(x-\tfrac{1}{4})(x-\tfrac{3}{4})\right)\cos\left(\pi(y-\tfrac{1}{4})(y-\tfrac{3}{4})\right), \end{aligned} \tag{5.17}$$

which corresponds to (Δt dependent) right hand sides $f = u_i - u_e - \Delta t I_m$. Note, that with (5.17) both $v \neq 0$ and $I_m \neq 0$. We discretize the domain by a uniform mesh by dividing the unit square into $n \times n$ squares and dividing each square by the (left) diagonal into isosceles triangles of size h, cf. Figure 5.1. To compare the dimensionality of the different formulations, Table 5.1 lists the dimensions of the four different finite element pairings over these meshes.

h	$\lvert V_{e,h}\rvert$	$\lvert V_{i,h}\rvert$	$\lvert Q_h\rvert$	$\lvert S_h\rvert$	$\lvert V_h\rvert$	$\lvert W_h\rvert$
4.42E-02	864	289	64	3136	2048	64
2.21E-02	3264	1089	128	12416	8192	128
1.10E-02	12672	4225	256	49408	32768	256
5.52E-03	49920	16641	512	197120	131072	512
2.76E-03	198144	66049	1024	787456	524288	1024
1.38E-03	789504	263169	2048	3147776	2097152	2048
6.93E-04	3151872	1050625	4096	12587008	8388608	4096

Table 5.1: Dimensions of the different finite element spaces for uniform refinements of the unit square. The first row corresponds to a mesh of Ω with $n = 16$, i.e. having $2 \times 16 \times 16$ cells.

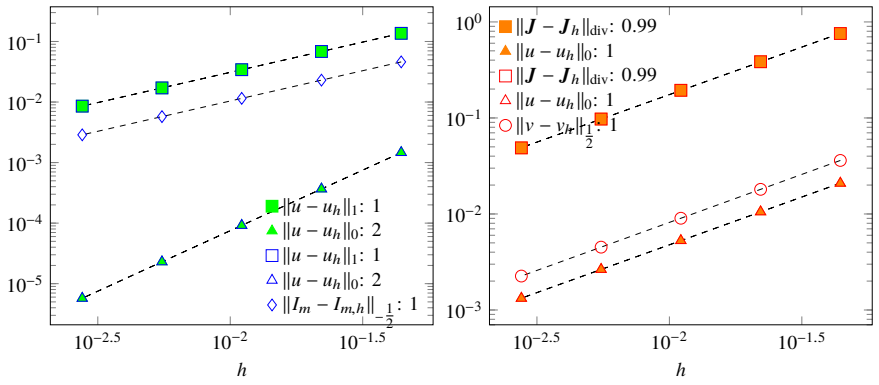

Fig. 5.2: Convergence properties of (left) primal formulations (5.6)–(5.8) and (right) mixed formulations (5.12)–(5.14). The EMI system (5.1) is solved with the exact solution given by (5.17) and $\Delta t = 1$. Filled symbols correspond to single-dimensional formulations. The number associated with each line indicates the convergence rate obtained from a least squares fit of the corresponding data.

On a series of meshes and for a set of different timesteps, we compute [2] the different approximations of all four finite element methods. We then evaluate the approximation error by evaluating the difference between (higher order interpolants of) the exact solution and the approximations in appropriate norms. Figure 5.2 shows the errors of the different formulations (with $\Delta t = 1$). In the primal formulations, u refers to the global potential, i.e. $u_i = u|_{\Omega_i}$, $u_e = u|_{\Omega_e}$. As the formulations seek the approximations $u_i \in H^1(\Omega_i)$, $u_e \in H^1(\Omega_e)$ the error is considered in the natural (broken) norm $\|u\|_1 = (\|u_i\|_1^2 + \|u_e\|_1^2)^{1/2}$. We observe that all the quantities converge linearly in their respective natural norms, as expected. In particular, the errors in the current density I_m in (5.8) and the transmembrane potential v in (5.14) are reported in the fractional norms $H^{-1/2}$ and $H^{1/2}$, respectively. The former is computed by first interpolating the error into the space of continuous piecewise cubic polynomials on Γ_h while for $v - v_h$ the P_1 element is used for error interpolation. Without this higher-order approximation of the error, i.e. if the error is computed in the same space as the discrete solution, we observe quadratic convergence.

Finally, we note that the primal formulations yield identical approximations of u cf. Figure 5.2 (left). Similarly, the mixed formulations give identical approximations of $(u, \boldsymbol{J})$ cf. Figure 5.2 (right). Considering for comparison the error in the potential in the L^2-norm, it can be seen that the primal formulations are more accurate than the mixed formulations. The same experiments for $\Delta t = 10^{-4}$ give similar approximation results. However, it is not true that these conclusions hold in the limit of Δt approaching 0, see e.g. Chapter 6.

5.5.2 Post-Processing the Transmembrane Potential

With the exception of the multi-dimensional mixed formulation (5.14), the transmembrane potential v in the remaining EMI formulations is computed by post-processing. In (5.6) the approximation v_h can be obtained by interpolating the difference $u_{i,h} - u_{e,h}$ onto e.g. the space of continuous piecewise linear functions over Γ_h. This procedure can, of course, be used in the other formulations as well. However (5.8) and (5.12) also offer an alternative approach. In the multi-dimensional primal formulation, the discrete membrane current density, $I_{m,h}$ is computed in the space $P_1(\Gamma_h)$ of continuous piecewise linear functions on Γ_h. In turn, v_h can be computed (in the same space) as a projection of $C_m^{-1}\Delta t I_{m,h} + f$. The same formula can be applied in the single-dimensional mixed formulation since the current density can be evaluated as $\boldsymbol{J}_h \cdot \boldsymbol{n}_i$. We recall that in (5.12) the natural space for v_h is the space of (discontinuous) piecewise constant functions on Γ_h however.

Convergence of the transmembrane potential obtained by the different formulations and post-processing strategies is shown in Figure 5.3 for the same test case as previ-

[2] The code used to produce results in this chapter is available at `https://github.com/MiroK/emi-book-fem` and archived at (12).

ously. We observe that the primal formulations yield quadratic convergence and that the single-dimensional primal (5.6), and multi-dimensional primal formulation (5.8) are practically identical. The discrete potentials obtained by solving the mixed formulations converge linearly with the projection method in the single-dimensional mixed formulation yielding the most accurate v_h. In particular, the approximation is better than that of the multi-dimensional mixed formulation for this test case. Computing the potential in the single-dimensional mixed formulation (5.12) by interpolating $u_{i,h} - u_{e,h}$ leads to poorer approximation than for the multi-dimensional mixed formulation. By comparing the results for two different time steps, we observe that the rates do not change considerably if Δt is modified.

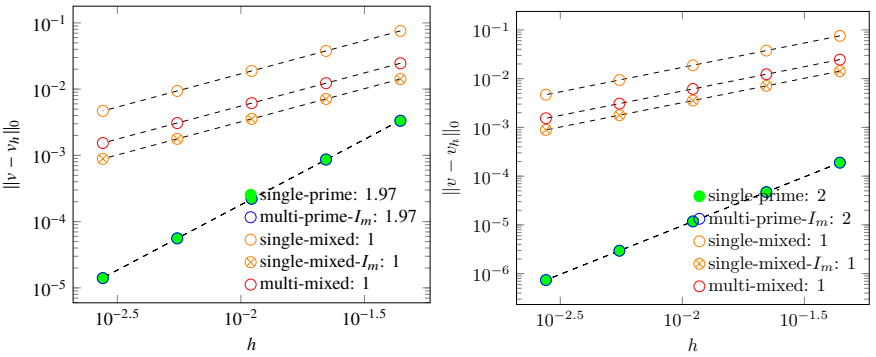

Fig. 5.3: Approximation of the transmembrane potential by the different EMI formulations. (Left) $\Delta t = 1$, (right) $\Delta t = 10^{-4}$. Postprocessing by projection (using the current density) is indicated by I_m. In multi-dimensional mixed formulation v_h is obtained by solving (5.14). Interpolation of $u_{i,h} - u_{e,h}$ is used in other formulations. The final number indicates the convergence rate.

5.6 Conclusions and Outlook

All four finite element formulations provide a converging approximation to the stationary problem (5.1). This system is a key building block in any operator splitting algorithm for the time-dependent EMI equations (1.30). The formulations provide solutions which differ by accuracy as well as computational cost, cf. Figures 5.2–5.3 and Table 5.1. The formulations also differ in robustness of their approximation properties with respect to Δt. This issue is however beyond the scope of this chapter, and the interested reader is referred to the discussion in Chapter 6. In terms of coupling with the membrane dynamics the single/multi-dimensional primal and single-dimensional mixed formulations require post-processing. However, all approaches discussed in Section 5.5.2 are easy to implement. Therefore, the choice of

which formulation to employ in solving the EMI model is largely a matter of desired accuracy and available computational resources.

References

1. Babuška I (1973) The finite element method with Lagrangian multipliers. Numerische Mathematik 20(3):179–192
2. Babuška I, Gatica GN (2003) On the mixed finite element method with Lagrange multipliers. Numerical Methods for Partial Differential Equations: An International Journal 19(2):192–210
3. Boffi D, Brezzi F, Fortin M, et al. (2013) Mixed Finite Element Methods and Applications, vol 44. Springer Berlin Heidelberg, Berlin, Heidelberg
4. Chandler-Wilde SN, Hewett DP, Moiola A (2015) Interpolation of Hilbert and Sobolev spaces: quantitative estimates and counterexamples. Mathematika 61(2):414–443
5. Evans LC (2010) Partial Differential Equations, vol 19. American Mathematical Soc., Providence, Rhode Island
6. Girault V, Raviart PA (2012) Finite Element Methods for Navier-Stokes Equations: Theory and Algorithms, vol 5. Springer Berlin Heidelberg, Berlin, Heidelberg
7. Jæger KH, Tveito A (2020) Derivation of a cell-based mathematical model of excitable cells. In: Tveito A, Mardal KA, Rognes ME (eds) Modeling Excitable Tissue - The EMI Framework, Simula Springer Notes in Computing, SpringerNature
8. Jæger KH, Hustad KG, Cai X, Tveito A (2020) Operator splitting and finite difference schemes for solving the EMI model. In: Tveito A, Mardal KA, Rognes ME (eds) Modeling Excitable Tissue - The EMI Framework, Simula Springer Notes in Computing, SpringerNature
9. Könnö J, Schötzau D, Stenberg R (2011) Mixed finite element methods for problems with Robin boundary conditions. SIAM Journal on Numerical Analysis 49(1):285–308
10. Kuchta M, Mardal KA (2020) Iterative solvers for cell-based EMI models. In: Tveito A, Mardal KA, Rognes ME (eds) Modeling Excitable Tissue - The EMI Framework, Simula Springer Notes in Computing, SpringerNature
11. Kuchta M, Nordaas M, Verschaeve JCG, Mortensen M, Mardal KA (2016) Preconditioners for saddle point systems with trace constraints coupling 2D and 1D domains. SIAM Journal on Scientific Computing 38(6):B962–B987
12. Kuchta M, Mardal KA, Rognes ME (2020) Software for EMI - Solving the EMI equations using finite element methods. DOI 10.5281/zenodo.3769254, URL `https://doi.org/10.5281/zenodo.3769254`
13. Wohlmuth BI (2000) A mortar finite element method using dual spaces for the Lagrange multiplier. SIAM Journal on Numerical Analysis 38(3):989–1012